Supporting Information

Tornberg et al. 10.1073/pnas.1102284108

SI Text

Human Pedigrees with IHH and *HS6ST1* Mutations. *Pedigree I.* The 55-y-old female proband with KS (no. 1) first presented at the age of 19 y with primary amenorrhea, congenital anosmia, obesity, a high-arched palate, bilateral genu valgus, and a medical history notable for osteoporosis (t score: <-3.0) with multiple vertebral and tibial fractures. Pituitary imaging [computed tomography (CT) scan] was normal, and an overnight frequent sampling study revealed lack of luteinizing hormone (LH) pulsatility, with a mean LH level of 5 IU/L, mean FSH level of 2 IU/L, and undetectable estradiol (Fig. S2). She presented at the age of 27 y seeking fertility and underwent ovulation induction with a physiological regimen of pulsatile GnRH (dose of 25 ng/kg), resulting in development of a single dominant follicle and ovulation but no conception. At the age of 39 y, she developed type 2 diabetes. Genetic screening revealed that the proband harbors three allelic defects, with a homozygous R296W/R296W mutation in *HS6ST1* and a heterozygous R250Q/+ mutation in *FGFR1*. The proband's family is French Canadian, and her pedigree is remarkable for several consanguineous loops as well as for several family members with IHH and associated phenotypes, including anosmia and cleft palate (1). The pedigree indicates an oligogenic pattern of inheritance, with affected subjects carrying two or more allelic defects. No phenotypic information is available on the proband's deceased father, who carries two allelic defects.

Pedigree II. The 10.5-y-old male proband with IHH (no. 2) was born with microphallus (stretched phallus length of 2.5 cm) but no cryptorchidism. At 4 mo of age, his serum hormonal levels were consistent with IHH (testosterone, <0.17 nmol/L; LH, 0.07 IU/L; FSH, 0.4 IU/L). Five days after a single i.m. injection of 2,900 U of hCG/m^2 of body surface area, plasma testosterone became detectable at 0.89 nmol/L. Three i.m. injections of testosterone enanthate (25 mg once a month) normalized phallus length (4.5 cm). MRI at 11 mo of age revealed a normal hypothalamic area and small pituitary, although the olfactory bulbs and nerves could not be assessed. Formal smell testing at the age of 7.5 y revealed hyposmia (score of 16/40, fifth percentile for sex and age). The proband's parents are first cousins. The mother also carries the *HS6ST1* R296Q mutation; she had delayed puberty (menarche at the age of 15 y) and reported a normal sense of smell.

Pedigree III. The 30-y-old male proband (no. 3) was born with congenital anosmia, a cleft palate, and bilateral genu valgus. He presented at the age of 15 y with prepubertal testes, anosmia, and undetectable gonadotropins with a frankly hypogonadal serum testosterone level (10 ng/dL). He was diagnosed with KS, and testosterone therapy was initiated. At the age of 22 y, he underwent a frequent sampling study that showed no LH pulses (Fig. S2) despite a hypogonadal serum testosterone level (115 ng/dL). MRI revealed absent olfactory bulbs and a normal pituitary, and a bone density scan showed mild osteopenia (t score of -1.6). One of the proband's two sisters carries the R313Q mutation but is reportedly asymptomatic and fertile, whereas the other sister exhibits anosmia but is WT for *HS6ST1* and also fertile. The proband's father carries the mutation and exhibited only delayed puberty, a less severe phenotype of GnRH deficiency. The paternal grandmother had delayed puberty, and the paternal grandfather was anosmic.

Pedigree IV. The 44-y-old male proband (no. 4) first presented at the age of 22 y with absent puberty and a decreased sense of smell (lower than fifth percentile for sex and age), consistent with KS. MRI showed normal pituitary and olfactory structures. Testosterone replacement was initiated, which induced normal virilization, libido, and potency. At the age of 35 y, he presented

seeking infertility; he had a testicular volume of 6 mL. An overnight frequent sampling study revealed a low-amplitude and low-frequency LH pulse pattern (3 pulses in 12 h, mean LH of 4.0 IU/L), low mean FSH of 2.8 IU/L, and a hypogonadal serum testosterone level (<100 ng/dL). Fertility induction with long-term pulsatile GnRH (maximum dose of 500 ng/kg) was successful, and he and his wife conceived three times. He also has osteoporosis (t score of -3.0). One of his brothers carries the identical *HS6ST1* mutation; he and/or his wife are infertile for unknown reasons, but he has a history of normal puberty and sense of smell.

Pedigree V. The 30-y-old male proband (no. 5) was born with microphallus and unilateral cryptorchidism. He was diagnosed with nIHH at the age of 21 y and was found to be osteopenic. Ultrasonography showed that both kidneys were normal. By the age of 25 y, his testicular volume was 15 mL bilaterally, consistent with a diagnosis of partial IHH. Notably, the proband's brother had delayed puberty, as evidenced by a late growth spurt and sparse shaving. Further detailed phenotyping was not feasible because the patient declined continued participation in the study.

Pedigree VI. The 42-y-old female proband with nIHH (no. 6) presented at the age of 16 y with primary amenorrhea and absent breast development. Her initial evaluation revealed delayed bone age (13.5 y at a chronological age of 16.5 y), a 46XX karyotype, normal pelvic ultrasound findings, normal brain and pituitary MRI scans, and a normal smell test result (score of 36/40, 28th percentile for sex and age), consistent with nIHH. A GnRH stimulation induced a modest increase in gonadotropins (LH level from undetectable to 4.7 IU/L, FSH level from 3.9 to 6.8 IU/L). She presented at the age of 23 y seeking fertility and underwent an overnight frequent blood sampling study showing undetectable LH and a mean FSH level of 3.69 IU/L. Pulsatile GnRH therapy (GnRH doses of 75–150 ng/kg at physiological frequencies) induced ovulation, and she conceived twice. The proband's 17-y-old daughter harbors the same mutation and has primary amenorrhea with a normal sense of smell, consistent with nIHH. The proband's twin sons are 13 y old, have WT *HS6ST1* sequences, and have entered puberty. The proband's brother, who is WT for *HS6ST1*, entered puberty late but developed fully by the age of 18 y. Notably, both of the proband's parents also had a history of delayed puberty.

Pedigree VII. The 36-y-old male proband with KS (no. 7) presented at the age of 21 y for failure to undergo puberty. He was anosmic, overweight (body mass index of 27) and eunuchoidal, and he had severe bilateral genu valgus. He had Tanner II pubic hair with a bilateral testicular size of 12–15 mL. A frequent sampling study revealed six pulses in 12 h with low amplitude (1.53 IU/L), a mean LH level of 3 IU/L, undetectable FSH, and a pooled serum T level of 17 ng/dL. His phenotype was consistent with partial KS, and he was treated with testosterone. While he was on replacement therapy, his wife conceived. Later, he was found to have a normal adult serum testosterone level and normal sperm count after having discontinued his replacement therapy, indicating reversal of his GnRH-deficiency IHH (2). His wife conceived a second child, and the patient underwent a vasectomy. Fourteen years later, a repeat neuroendocrine study revealed a normal LH pulse pattern (7 pulses in 12 h, mean amplitude of 4.40 IU/L, mean LH level of 9.86 IU/L, mean FSH level of 2.51 IU/L) and an adult serum testosterone level of 394 ng/dL, confirming a sustained reversal of his GnRH deficiency. Interestingly, his MRI scan showed absent olfactory bulbs and a small pituitary gland. The proband's maternal grandparents were first cousins; one of his daughters is obese with developmental delays at the age of 8 y.

SI Materials and Methods

Phenotyping and Genotyping of the IHH Cohort. *Phenotyping.* IHH was defined as absent or incomplete puberty by the age of 18 y, with low serum gonadotropin levels. Males had low serum testosterone levels (<100 ng/dL, reference range: 280–1,100 ng/dL), and females had hypoestrogenic primary amenorrhea. Detailed histories were obtained and physical examinations were performed as previously reported (3). Proband 2 was diagnosed earlier in life because of microphallus and undetectable gonadotropins during the first 6 mo of age (4). All subjects had normal pituitary reserve function and no structural anomalies of the pituitary-hypothalamic area by MRI or CT scan. KS was defined as IHH with anosmia or hyposmia by history and was confirmed by means of the University of Pennsylvania Smell Identification Test (UPSIT) (3). A UPSIT score less than or equal to the fifth percentile for sex and age was considered hyposmia, and a total score ≤16/40 was considered anosmia. When possible, GnRH deficiency was assessed by an overnight study of LH secretion pattern, with blood sampling every 10 min for 12 h.

Genotyping. All subjects and available family members were screened for mutations in the *KAL1, GNRHR, NELF, GPR54, PROK2, PROKR2, FGFR1,* and *FGF8* genes as previously described (3, 5–11) as well as for mutations in *HS6ST1.* The exon-intron structure and nucleotide sequence of *HS6ST1* (NM_004807) were identified using the University of California, Santa Cruz (http://www.genome.ucsc.edu) and ENSEMBL (http://www.ensembl.org) genome databases. DNA sequencing of the two coding exons and splice junctions of *HS6ST1* was performed after PCR amplification with gene-specific primers (Table S2). Nonsynonymous sequence changes were defined as mutations if they were absent from 500 ethnically and age-matched controls and rom the SNP database (http://www.ncbi.nlm.nih.gov/projects/SNP/). All sequence variations were confirmed by sequencing both strands from at least two independent PCR reactions. The Human Research Committee of Massachusetts General Hospital approved this study, and all subjects provided written informed consent before participation.

In Vitro and in Vivo Assays for *HS6ST1* Activity. *Production of recombinant HS6ST1 protein.* The human HS6ST1 cDNA (IMAGE consortium accession ID BC099638) was obtained from Open Biosystems. The HS6ST1 R296W, R296Q, R313Q, R372W, and M394V point mutations were introduced using PCR-mediated mutagenesis (Quickchange II; Stratagene) and verified by sequencing. WT and mutant human *HS6ST1* cDNAs were ligated into the *Kpn*I/*Xba*I sites of the pFLAG–CMV-2 expression vector (Sigma), and the final constructs were confirmed by sequencing. Transfection of cDNAs and transient expression of human *HS6ST1* and its mutants in COS-7 cells were carried out as described previously (12). Briefly, the cells (1×10^6) were seeded into 60-mm dishes; cultured in DMEM containing 10% (vol/vol) FBS for 24 h; and transfected with 4 μg of pFLAG–CMV-2 hHS6ST1, mutant plasmids of pFLAG–CMV-2 hHS6ST1, and pFLAG–CMV-2 alone using TrasFast (Promega) according to the manufacturer's recommendations. Cells were incubated in DMEM supplemented with 10% (vol/vol) FBS and antibiotics for 48 h. Cell layers were washed with DMEM, scraped, and homogenized in 1 mL of 10 mM Tris/HCl (pH 7.2), 0.5% (wt/vol) Triton X-100, 0.15 M NaCl, 20% (wt/vol) glycerol, 10 mM $MgCl_2$, and 2 mM $CaCl_2$. The homogenates were stirred for 1 h and then centrifuged at $10,000 \times g$ for 30 min at 4 °C. HS6ST1-FLAG fusion proteins were isolated from the supernatant (cell extract) by anti-FLAG M2 affinity chromatography (Sigma) according to the manufacturer's instructions. The amount of FLAG-tagged proteins was determined by Western blotting (ECL detection system) using an anti-FLAG antibody and densitometry in a lumino image analyzer (LAS-4000 miniEPUV; Fujifilm) (Fig. S3).

In vitro assay for HS6ST1 activity. Sulfotransferase activities were determined as described previously (12). Briefly, the standard reaction mixture (50 μL) contained 2.5 μmol of imidazole-HCl (pH 6.8); 3.75 μg of protamine chloride; 2.5, 5, and 25 nmol (as hexosamine) of CDSNS-heparin or HS (from pig aorta) as the acceptor substrate, 50 pmol of [S^{35}]-labeled phosphoadenosyl-phosphosulfate (PAPS; approximately 7×10^5 cpm), and recombinant HS6ST1 enzyme. After incubation for 20 min at 37 °C, the reaction was stopped by heating at 100 °C for 1 min. Carrier chondroitin sulfate A (0.1 μmol as GlcA) was added to the reaction mixture, and the [S^{35}]-labeled acceptor substrates were isolated by precipitation with ethanol containing 1.3% (wt/vol) potassium acetate and 0.5 mM EDTA, followed by gel chromatography on a Fast Desalting column to remove [S^{35}]-labeled PAPS and its degradation products. One unit of enzyme activity was defined as the amount required to transfer 1 pmol of sulfate per minute to the acceptor substrate. Relative enzymatic activities were calculated by normalizing to the total amount of protein (Fig. S3).
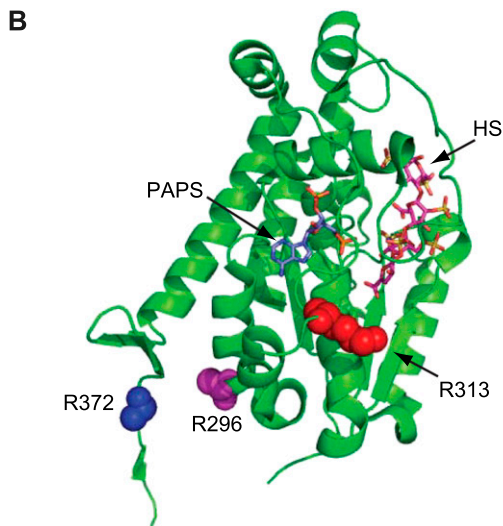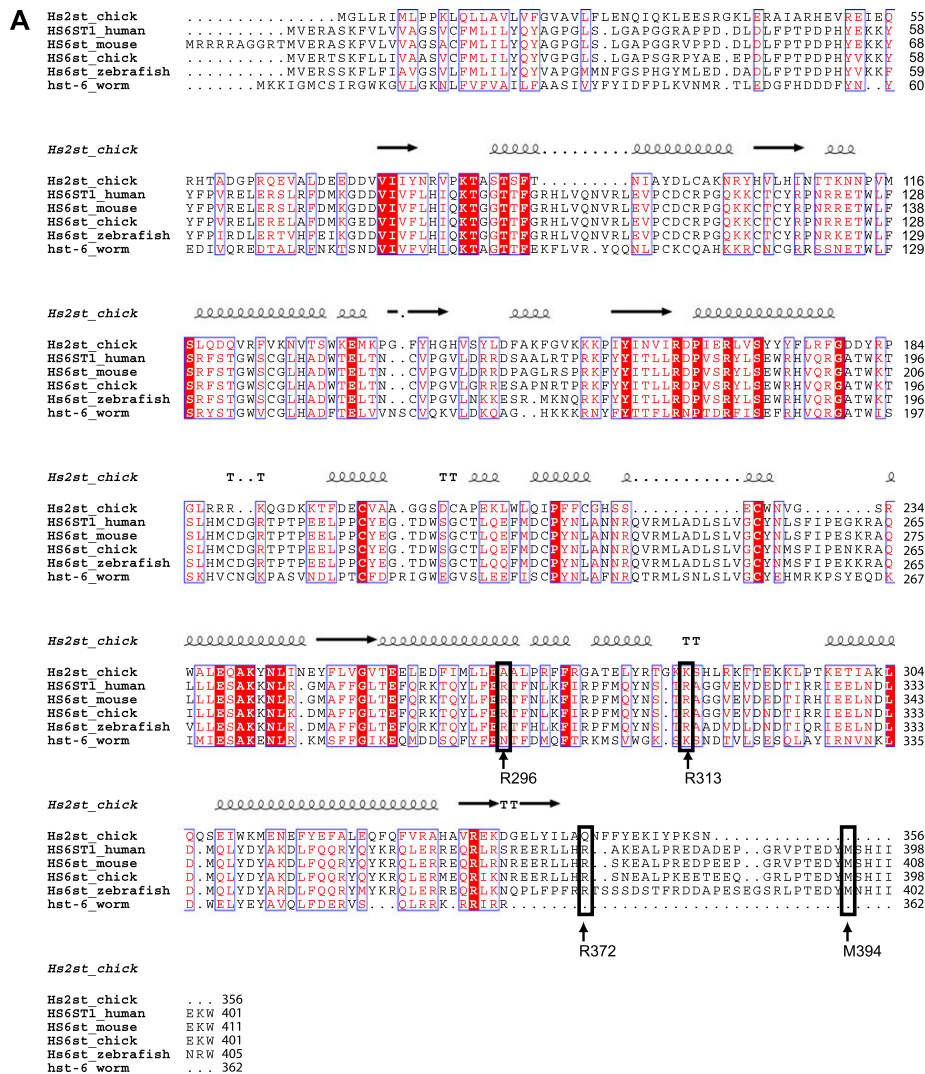
In vivo assay for human HS6ST1 activity in C. elegans. Standard methods were used for handling and culturing *C. elegans* (13). The human *HS6ST1* cDNA (IMAGE consortium accession ID BC099638) was obtained from Open Biosystems. The *HS6ST1* R296W, R296Q, R313Q, R372W, and M394V point mutations were generated using the Quickchange II Site-Directed Mutagenesis Kit (Stratagene). All constructs were verified by sequencing. *HS6ST1* WT and mutant cDNAs were cloned between the *Kpn*I/*Pfo*I restriction sites into *phst-6::gfp* (14) to express the cDNA under the control of the *C. elegans hst-6* promoter. To create transgenic animals, constructs were injected at a concentration of 2.5 ng/μL into *otIs76mgIs18; hst-6 (ok273)* (14), with *pRF4 (rol-6(su1006))* at a concentration of 100 ng/μL as a dominant injection marker. Neuroanatomy was scored as described (14). Statistical significance was calculated using the *z* test, and values were subjected to the Bonferroni correction where applicable. Percent decrease of rescuing activity was calculated by assigning the difference between baseline branching in *hst-6* mutants and the average of five lines expressing the *HS6ST1* WT cDNA under the *hst-6* promoter as 100%.

Transgenic rescue of AFD branching. For rescue of AFD branching, the cDNAs of egl-15(A) or egl-17 were cloned under control of both the dpy-7 and gcy-8 promoters (41, 42). Constructs were injected at 10 ng/L, together with 50 ng/L each of *punc-122::GFP* (which labels the easily identifiable coelomocytes) and *pBS* into *otIs83 oyIs17*; *egl-15(n484)* or *otIs83 oyIs17*; *egl-17(n1377)* as applicable. The *otIs83 oyIs17* is a strain that both visualizes AFD neurons with GFP and overexpresses *kal-1* (21).

Quantitative Real-Time PCR. Total RNA from 50 adult worms was extracted using the RNeasy Micro Kit (Qiagen). First-strand cDNA synthesis was performed using the SuperScript III First-Strand Synthesis System (Invitrogen). Real-time PCR was performed with specific primers for human *HS6ST1* using the PowerSYBR Green Mastermix Kit and the ABI prism 7700 Sequence Detection System (both from Applied Biosystems). Denaturation, annealing, and extension were repeated 40 times as follows: 95 °C for 10 s, 60 °C for 20 s, and 72 °C for 30 s. All reactions were performed in triplicate. The specificity of amplification was confirmed by melt-curve analysis. The relative quantities of transcripts were calculated and normalized to the expression of the ρ-GTPase *cdc-42* (15, 16).

Molecular Modeling. High-resolution crystal structures have been determined for three distinct HS sulfotransferases: NDST1, HS 2-*O*-sulfotransferase (HS2ST), and HS3ST1. These structures form the basis of modeling the potential effects of the *HS6ST1* alleles reported here. Of the three known structures, human HS6ST1 most closely resembles HS2ST (not shown). The model of HS6ST1 shown in Fig. S1*B* is based on the HS2ST crystal structure (17), and the structural alignment shown in Fig. S1*A*. The model was manipulated using PyMol (18).

1. White BJ, Rogol AD, Brown KS, Lieblich JM, Rosen SW (1983) The syndrome of anosmia with hypogonadotropic hypogonadism: A genetic study of 18 new families and a review. *Am J Med Genet* 15:417–435.
2. Raivio T, et al. (2007) Reversal of idiopathic hypogonadotropic hypogonadism. *N Engl J Med* 357:863–873.
3. Pitteloud N, et al. (2006) Mutations in fibroblast growth factor receptor 1 cause both Kallmann syndrome and normosmic idiopathic hypogonadotropic hypogonadism. *Proc Natl Acad Sci USA* 103:6281–6286.
4. Grumbach MM (2005) A window of opportunity: The diagnosis of gonadotropin deficiency in the male infant. *J Clin Endocrinol Metab* 90:3122–3127.
5. Cole LW, et al. (2008) Mutations in prokineticin 2 and prokineticin receptor 2 genes in human gonadotrophin-releasing hormone deficiency: Molecular genetics and clinical spectrum. *J Clin Endocrinol Metab* 93:3551–3559.
6. Falardeau J, et al. (2008) Decreased FGF8 signaling causes deficiency of gonadotropin-releasing hormone in humans and mice. *J Clin Invest* 118:2822–2831.
7. Oliveira LM, et al. (2001) The importance of autosomal genes in Kallmann syndrome: Genotype-phenotype correlations and neuroendocrine characteristics. *J Clin Endocrinol Metab* 86:1532–1538.
8. Pitteloud N, et al. (2005) Reversible kallmann syndrome, delayed puberty, and isolated anosmia occurring in a single family with a mutation in the fibroblast growth factor receptor 1 gene. *J Clin Endocrinol Metab* 90:1317–1322.
9. Pitteloud N, et al. (2007) Digenic mutations account for variable phenotypes in idiopathic hypogonadotropic hypogonadism. *J Clin Invest* 117:457–463.
10. Seminara SB, et al. (2000) Successful use of pulsatile gonadotropin-releasing hormone (GnRH) for ovulation induction and pregnancy in a patient with GnRH receptor mutations. *J Clin Endocrinol Metab* 85:556–562.
11. Seminara SB, et al. (2003) The GPR54 gene as a regulator of puberty. *N Engl J Med* 349:1614–1627.
12. Habuchi H, et al. (2000) The occurrence of three isoforms of heparan sulfate 6-O-sulfotransferase having different specificities for hexuronic acid adjacent to the targeted N-sulfoglucosamine. *J Biol Chem* 275:2859–2868.
13. Brenner S (1974) The genetics of Caenorhabditis elegans. *Genetics* 77:71–94.
14. Bülow HE, Hobert O (2004) Differential sulfations and epimerization define heparan sulfate specificity in nervous system development. *Neuron* 41:723–736.
15. Hoogewijs D, Houthoofd K, Matthijssens F, Vandesompele J, Vanfleteren JR (2008) Selection and validation of a set of reliable reference genes for quantitative sod gene expression analysis in C. elegans. *BMC Mol Biol* 9:1–9.
16. Pfaffl MW (2001) A new mathematical model for relative quantification in real-time RT-PCR. *Nucleic Acids Res* 29:e45.
17. Bethea HN, Xu D, Liu J, Pedersen LC (2008) Redirecting the substrate specificity of heparan sulfate 2-O-sulfotransferase by structurally guided mutagenesis. *Proc Natl Acad Sci USA* 105:18724–18729.
18. The PyMOL Molecular Graphics System, Version 1.3, Schrödinger, LLC.
19. Subramaniam S (1998) The Biology Workbench—A seamless database and analysis environment for the biologist. *Proteins* 32:1–2.
20. Gouet P, Courcelle E, Stuart DI, Métoz F (1999) ESPript: Analysis of multiple sequence alignments in PostScript. *Bioinformatics* 15:305–308.
21. Bülow HE, Berry KL, Topper LH, Peles E, Hobert O (2002) Heparan sulfate proteoglycan-dependent induction of axon branching and axon misrouting by the Kallmann syndrome gene kal-1. *Proc Natl Acad Sci USA* 99:6346–6351.
22. Gilleard JS, Barry JD, Johnstone IL (1997) cis regulatory requirements for hypodermal cell-specific expression of the Caenorhabditis elegans cuticle collagen gene dpy-7. *Mol Cell Biol* 17:2301–2311.
23. Yu S, Avery L, Baude E, Garbers DL (1997) Guanylyl cyclase expression in specific sensory neurons: A new family of chemosensory receptors. *Proc Natl Acad Sci USA* 94:3384–3387.

A

```
Hs2st_chick     ...............MGLLRIMLPPKLQLLAVLVFGVAVLFLENQIQKLEESRGKLERAIARHEVREIEQ   55
HS6ST1_human    ..........MVERASKFVLVVAGSVCFMLILYQYAGPGLS.LGAPGGRAPPD.DLDLFPTPDPHYEKKY   58
HS6st_mouse     MRRRRAGGRTMVERASKFVLVVAGSACFMLILYQYAGPGLS.LGAPGGRVPPD.DLDLFPTPDPHYEKKY   68
HS6st_chick     ..........MVERTSKFLLIVAASVCFMLILYQYVGPGLS.LGAPSGRPYAE.EPDLFPTPDPHYVKKY   58
Hs6st_zebrafish ..........MVERSSKFLFIAVGSVLFMLILYQYVAPGMMNFGSPHGYMLED.DADLFPTPDPHYVKKF   59
hst-6_worm      .......MKKIGMCSIRGWKGVLGKNLFVFVAILFAASIVYFYIDFPLKVNMR.TLEDGFHDDDFYN..Y   60
```

Hs2st_chick

```
Hs2st_chick     RHTADGPRQEVALDEEDDVVIIYNRVPKTASTSFT.........NIAYDLCAKNRYHVLHINTTKNNPVM  116
HS6ST1_human    YFPVRELERSLRFDMKGDDVIVFLHIQKTGGTTFGRHLVQNVRLEVPCDCRPGQKKCTCYRPNRRETWLF  128
HS6st_mouse     YFPVRELERSLRFDMKGDDVIVFLHIQKTGGTTFGRHLVQNVRLEVPCDCRPGQKKCTCYRPNRRETWLF  138
HS6st_chick     YFPVRELERELAFDMKGEDVIVFLHIQKTGGTTFGRHLVQNVRLEVPCDCRPGQKKCTCYRPNRRETWLF  128
Hs6st_zebrafish YFPIRDLERTVHFEIKGDDVIVFLHIQKTGGTTFGRHLVQNVRLEVPCDCRPGQKKCTCYRPNRRETWLF  129
hst-6_worm      EDIVQREDTALRFNKTSNDVIVFVHIQKTAGTTFREKFLVR.YQQNLPCKCQAHKKRCNCGRRSSNETWLF  129
```

Hs2st_chick

```
Hs2st_chick     SLQDQVRFVKNVTSWKEMKPG.FYHGHVSYLDFAKFGVKKKPIYINVIRDPIERLVSYYYFLRFGDDYRP  184
HS6ST1_human    SRFSTGWSCGLHADWTELTN..CVPGVLDRRDSAALRTPRKFYITLLRDPVSRYLSEWRHVQRGATWKT   196
HS6st_mouse     SRFSTGWSCGLHADWTELTN..CVPGVLDRRDPAGLRSPRKFYITLLRDPVSRYLSEWRHVQRGATWKT   206
HS6st_chick     SRFSTGWSCGLHADWTELTN..CVPGVLGRRESAPNRTPRKFYITLLRDPVSRYLSEWRHVQRGATWKT   196
Hs6st_zebrafish SRFSTGWSCGLHADWTELTN..CVPGVLNKKESR.MKNQRKFYITLLRDPVSRYLSEWRHVQRGATWKT   196
hst-6_worm      SRYSTGWVCGLHADFTELVVNSCYQKVLDKQAG..HKKKRNYFYTTFLRNPTDRFISEFRHVQRGATWLS   197
```

Hs2st_chick

```
Hs2st_chick     GLRRR..KQGDKTFDBCVAA.GGSDCAPEKLWLQIPFFCGHSS...........ECWNVG.......SF   234
HS6ST1_human    SLHMCDGRTPTPEELPPCYEG.TDWSGCTLQEFMDCPYNLANNRQVRMLADLSLVGCYNLSFIPEGKRAQ  265
HS6st_mouse     SLHMCDGRTPTPEELPPCYEG.TDWSGCTLQEFMDCPYNLANNRQVRMLADLSLVGCYNLSFIPESKRAQ  275
HS6st_chick     SLHMCDGRTPTPEELPSCYEG.TDWSGCTLQEFMDCPYNLANNRQVRMLADLSLVGCYNMSFIPENKRAQ  265
Hs6st_zebrafish SLHMCDGRTPTPEELPPCYEG.TDWSGCTLQQFMDCPYNLANNRQVRMLADLSLVGCYNMSFIPEKKRAQ  265
hst-6_worm      SKHVCNGKPASVNDLPTCFDPRIGWEGVSLEEFISCDYNLAFNRQTRMLSNLSLVGCYEHMRKPSYEQDK  267
```

Hs2st_chick

```
Hs2st_chick     WALEQAKYNLINEYFLVGVTEELEDFIMLLEALPRPRGATELYRTGKKSHLRKITEKKLPTKETIAKL   304
HS6ST1_human    LLLESAKNLR.GMAFFGLTEFQRKTQYLPFRTFNLKPIRPFMQYNS.IRAGGVEVDEDTIRRIEELNDL  333
HS6st_mouse     LLLESAKNLR.GMAFFGLTEFQRKTQYLPFRTFNLKPIRPFMQYNS.IRAGGVEVDEDTIRHIEELNDL  343
HS6st_chick     LLLESAKNLK.DMAFFGLTEFQRKTQYLPFRTFNLKPIRPFMQYNS.IRAGGVEVDNDTIRRIEELNDL  333
Hs6st_zebrafish VLLESAKNLR.DMAFFGLTEFQRKTQYLPFRTFHLKPIRPFMQYNS.IRAADVDLDNDTIQRIEELNDL  333
hst-6_worm      IMIESAKENLR.KMSFFGIKEQMDDSQFYPFRTFDMQFTRKMSVWGK.SFNDTVLSESQLAYLRNVNKL  335
```
R296   R313

Hs2st_chick

```
Hs2st_chick     QQSEIWKMENEFYEFALEQFQFVRAHAVREKDGELYILAQNFFYEKIYPKSN..............   356
HS6ST1_human    D.MQLYDYAKDLFQQRYQYKRQLERREQRLRSREERLLHR..AKEALPREDADEP..GRVPTEDYMSHII  398
HS6st_mouse     D.MQLYDYAKDLFQQRYQYKRQLERREQRLRNREEARLLR..SKEALPREDPEEP..GRVPTEDYMSHII  408
HS6st_chick     D.MQLYDYAKDLFQQRYQYKRQLERMEQRIKNREERLLHR..SNEALPKEETEEQ..GRLPTEDYMSHII  398
Hs6st_zebrafish D.MQLYDYARDLFQQRYMYKRQLERREQRLKNQPLFFPFR.SSSDSTFRDDAPESEGSRLPTEDYMNHII  402
hst-6_worm      D.WELYEYAVQLFDERVS...QLRRK.RRIRR.................................   362
```
R372   M394

Hs2st_chick

```
Hs2st_chick     ...  356
HS6ST1_human    EKW  401
HS6st_mouse     EKW  411
HS6st_chick     EKW  401
Hs6st_zebrafish NRW  405
hst-6_worm      ...  362
```

B

Fig. S1. (*A*) Protein sequence alignment of HS sulfotransferases. Primary protein sequence alignments were performed using Biology Workbench (http://workbench.sdsc.edu/) (19). The validity of the alignment was assessed manually by superimposing the structure of HS 2-*O*-sulfotransferase (PDB ID code 3F5F) and HS 3-*O*-sulfotransferase (PDB ID code 1T8U). The alignments were graphically rendered, and the structure of chick HS 2-*O*-sulfotransferase (PDB ID code 3F5F) was superimposed using ESPript (20). When human HS6ST2 is included in the sequence alignment, the projected position of the R313 residue shifts seven amino acids toward the C terminus in the HS 2-*O*-sulfotransferase structure (not shown). This position of R313 is consistent with a role in PAPS and/or substrate recognition. Structural elements, such as α-helices, turns (T), and β-strands (arrows), are indicated. Amino acid positions are denoted on the right. HS2ST, HS 2-*O*-sulfo-

transferase; HS3ST, HS 3-*O*-sulfotransferase. (*B*) 3D model of human HS6ST1 based on sequence alignments and the crystal structure of the HS 2-*O*-sulfotransferase (3F5F) and HS 3-*O*-sulfotransferase (1T8U). The R296 residue (magenta) maps near a turn at the base of a short helix that makes direct contact with the PAPS cofactor (stick model shown in blue and red). Thus, mutation of R296 could affect binding of PAPS to the enzyme. R313 (red) localizes near the site of catalysis between the HS substrate and PAPS. Mutation of this residue could affect binding of HS and/or PAPS (stick model shown in magenta and red). R372 (blue) is located in a strand of the protein predicted to make contact with an adjacent protomer in the functional trimer of vertebrate HS sulfotransferases. Residues in this strand are required for the enzymatic activity of HS 2-*O*-sulfotransferase (17). The M394 residue lies outside of the crystallized domain and is not part of this model.
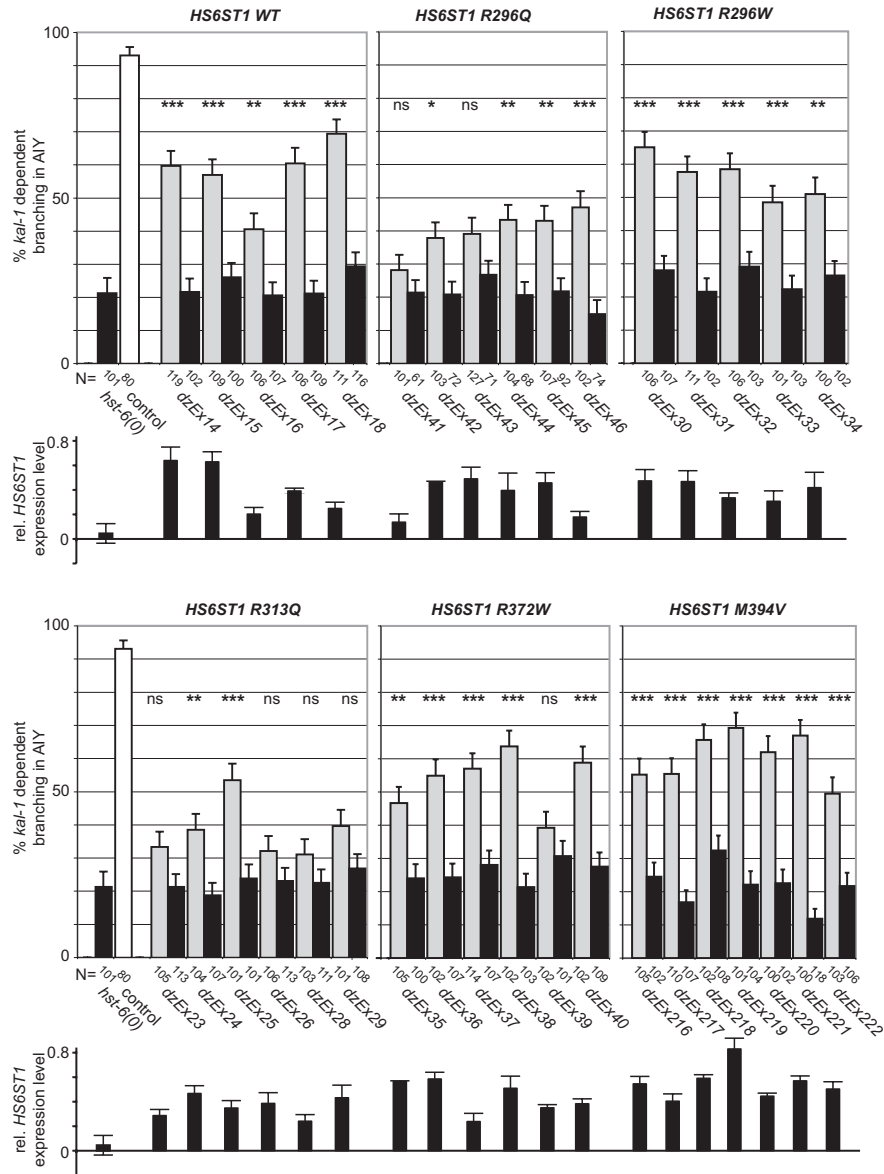

Fig. S2. Individual transgenic lines for the *HS6ST1* in vivo assay. The *kal-1*–dependent axon branching phenotype was quantified in individual transgenic lines expressing point mutant versions of *HS6ST1*. A white bar shows the *kal-1* gain-of-function–dependent branching phenotype in a WT genetic background, and black bars show the branching phenotype in a *C. elegans hst-6* null mutant background. Gray bars represent the *kal-1*–dependent branching phenotype in the presence of various transgenes comprising WT and point mutant versions of the human *HS6ST1* cDNA as indicated. All black bars directly adjacent to gray bars display the branching phenotype in nontransgenic siblings of animals expressing the respective human *HS6ST1* cDNA constructs. The transcript levels of transgenic *HS6ST1* relative to endogenous *cdc-42* expression are indicated as a bar graph below each transgenic line and represent the average of two or more independent experiments. rel., relative.
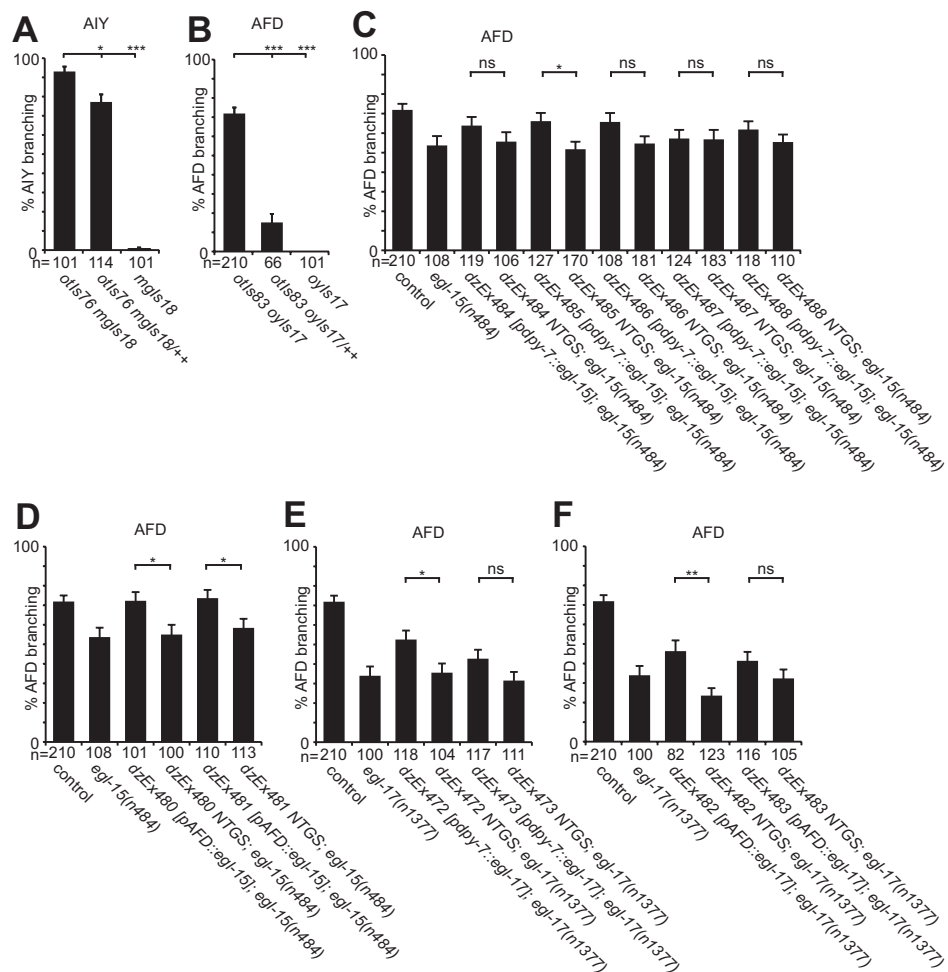
Fig. S3. *kal-1*–dependent phenotypes in AIY and AFD neurons are molecularly distinct. (*A*) *kal-1*–dependent branching phenotype in AIY interneurons is dosage-sensitive. *otIs76* is a transgene that expresses *kal-1*, and *mgIs18* is a transgene that expresses GFP under control of the AIY-specific *ttx-3* promoter (21). (*B*) *kal-1*–dependent branching phenotype in AFD sensory neurons is dosage-sensitive. The *otIs83* and *oyIs17* transgenes express *kal-1* and GFP, respectively, under control of the AFD-specific *gcy-8* promoter (21). (*C*) Transgenic expression of the FGFR/*egl-15* receptor in the hypodermis (using the *dpy-7* promoter) (22) fails to rescue the *kal-1*–dependent phenotype in AFD neurons. NTGS, nontransgenic siblings of extrachromosomal (Ex) transgenic lines as indicated. The data for control, *egl-17*, or *egl-15* in *C–F* are the same as in Fig. 3 and are shown for comparison only. (*D*) Transgenic expression of the FGFR/*egl-15* receptor in AFD neurons (using the *gcy-8* promoter) (23) fully rescues the *kal-1*–dependent phenotype in AFD neurons. (*E*) Transgenic expression of the FGF/*egl-17* ligand in the hypodermis (using the *dpy-7* promoter) (22) partially rescues the *kal-1*–dependent phenotype in AFD neurons. (*F*) Transgenic expression of the FGF/*egl-17* ligand in AFD neurons (using the *gcy-8* promoter) (23) partially rescues the *kal-1*–dependent phenotype in AFD neurons.
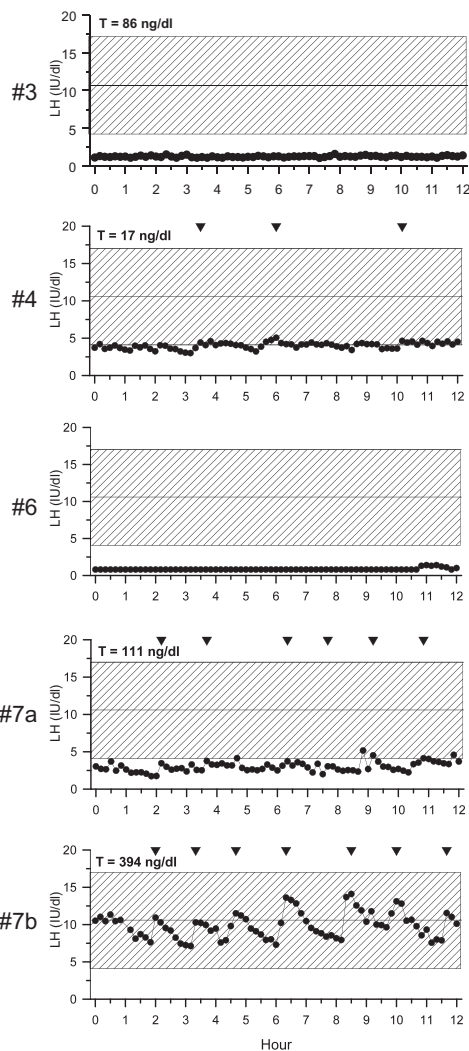
Fig. S4. Patients with *HS6ST1* mutations display a spectrum of LH release patterns. LH is released by the pituitary in response to stimulation by hypothalamic GnRH. LH serum levels were determined by overnight frequent sampling as surrogates for GnRH secretion. The hatched area denotes the normal range of LH levels, and arrowheads indicate LH pulses. Probands 3 and 6 are apulsatile, whereas probands 4 and 7 have pulses of subnormal amplitude. 7a and 7b show the LH release patterns of proband 7 before (*a*) and after (*b*) his spontaneous reversal of IHH. T, Testosterone.
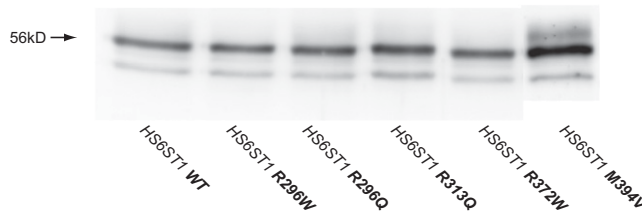
Fig. S5. Relative quantification of recombinant HS6ST1 proteins. The purified recombinant protein (50 μL) was precipitated with 2.5 volumes of cold ethanol containing 1.3% (w/v) potassium acetate. The precipitates were analyzed by Western blot as described in *Materials and Methods*. The relative amount of protein was quantified by a lumino image analyzer (LAS-4000 mini EPUV; Fujifilm). The arrow indicates the major band of 56 kDa of HS6ST1-FLAG. Lane 1, WT HS6ST1 (relative amount = 1.0); lane 2, R296W (relative amount = 0.95); lane 3, R296W (relative amount = 1.13); lane 4, R313Q (relative amount = 1.23); and lane 5, R372W (relative amount = 1.03). The experiment was repeated with comparable results (not shown).

Table S1. Clinical presentation of patients with *HS6ST1* mutations

Proband no.	Sex	Diagnosis	Puberty	Other phenotypes	*HS6ST1* genotype	Other gene defects
1	♀	KS	Absent	High-arched palate, osteoporosis, fractures, bilateral genu valgus, obesity, type 2 diabetes	R296W/R296W	*FGFR1* R250Q/+
2	♂	KS	Prepubertal		R296Q/+	ND
3	♂	KS	Absent	Cleft palate, osteopenia, bilateral genu valgus	R313Q/+	ND
4	♂	KS	Partial	Osteoporosis	R372W/+	*NELF* T480A/+
5	♂	nIHH	Partial	Osteopenia	R372W/+	ND
6	♀	nIHH	Absent		R372W/+	ND
7	♂	KS	Partial	Bilateral genu valgus	M394V/+	ND

KS, IHH with anosmia; +, wild type allele; ND, no mutations detected in *KAL1, GNRHR, NELF, GPR54, PROK2, PROKR2, FGFR1*, or *FGF8* gene.

Table S2. Primers used to amplify *HS6ST1* sequences

HS6ST1 primers for sequencing exon 1 and exon 2

Exon 1-F: 5′-CTG AGG GCG GAA TCA CTT C-3′
Exon 1-R: 5′-GCC GAC CCA GTA CAG CAC-3′
Annealing temperature: 60 °C
5% (v/v) DMSO
Exon 2-F: 5′-GTC ACA GCC CTC ACC TCC T-3′
Exon 2-R: 5′-GTC CTG TTT TAT CCC CCA CA-3′
Annealing temperature: 64 °C
5% (v/v) DMSO

HS6ST1 primers for quantitative RT-PCR
HB432: 5′-GAG AGC GCC AAG AAG AAC CTG-3′
HB433: 5′-ATG AAG GGC CGG ATG AAC TTG-3′

cdc-42 primers for quantitative RT-PCR
HB430: 5′-CTG CTG GAC AGG AAG ATT ACG-3′
HB431: 5′-CTC GGA CAT TCT CGA ATG AAG-3′